Computational Mechanics 14 (1994) 354–369 © Springer-Verlag 1994

Dynamic shear band development in dipolar thermoviscoplastic materials

R. C. Batra, J. Hwang

Abstract We study thermomechanical deformations of a viscoplastic body deformed in plane strain compression at a nominal strain-rate of 5000 $\sec^{-1}$. We develop a material model in which the second order gradients of the velocity field are also included as kinematic variables and propose constitutive relations for the corresponding higher order stresses. This introduces a material characteristic length l, in addition to the viscous and thermal lengths, into the theory. It is shown that the computed results become mesh independent for l greater than a certain value. Also, the consideration of higher order velocity gradients has a stabilizing effect in the sense that the initiation of shear bands is delayed and their growth is slower as compared to that for nonpolar ($l = 0$) materials.

1 Introduction

Since the early 1980's there has been a significant increase in research activity in the area of shear banding in materials deformed at high strain rates. Shear bands, which are narrow regions of intense plastic deformation have been termed adiabatic since, at high rates of deformation, there is not enough time for the heat to be conducted away. However, heat transfer out of the hotter severely deformed region probably plays an important role in controlling the width of these bands.

Tresca (1878) was the first to observe these shear bands during the forging of a platinum bar. He termed these hot lines and stated that these were the lines of greatest development of heat. Subsequently, Massey (1921) observed these hot lines during the hot forging of a metal, and stated that "when diagonal 'slipping' takes place, there is a great friction between particles and a considerable amount of heat is generated." Zener and Hollomon (1944) reported 32 μm wide shear bands during the punching of a hole in a steel plate and asserted that the heat generated because of plastic working softened the material and that the material became unstable when thermal softening equalled the combined effects of strain and strain-rate hardening. The reader is referred to the recent book by Bai and Dodd (1992) for numerous references on the subject.

The study of shear bands in a thermoviscoplastic body being deformed in simple shear (e.g., see Batra (1992)) has revealed that peak strain gradients of the order of 0.2 per μm occur in the vicinity of the shear band. Motivated by such considerations, Wright and Batra (1987) proposed a one-dimensional theory for rate dependent dipolar materials by modifying the dipolar theory of Green et al. (1968) to include rate effects, and showed that the consideration of second order gradients of the velocity field delayed the initiation of the shear band. Here we first generalize the dipolar theory of Green et al. (1968) to rate-dependent materials, and then use it to study the phenomenon of shear banding in a body made of such a material and deformed in plane strain compression. Our formulation of the problem differs from that of de Borst (1991), who used the Cosserat (1909) theory and included rotations and the corresponding

Communicated by S. N. Atluri, 7 March 1994

R. C. Batra, J. Hwang
Department of Mechanical and Aerospace, Engineering and Engineering Mechanics, University of Missouri-Rolla, Rolla, MO 65401-0249, USA

R. C. Batra
Present address: Clifton G. Garvin Professor, Dept. of Engng. Sci & Mechs., Virginia Polytechnic Institute & State Univ., Blacksburg, VA 24061-0219, USA

This work was supported by the U.S. Army Research Office grant DAAL03-91-G-0084 and the NSF grant MSS9121279 to the University of Missouri-Rolla. Some of the computations were performed on the Ohio Supercomputer center in Columbus, Ohio

higher order stresses into the theory. Dillon and Kratochvil's (1970) motivations in proposing a higher order gradient theory of infinitesimal deformations plasticity were: 1) the basic concept of work hardening due to Seeger (1957) in which dislocations interact and, therefore, the internal forces are not restricted to being of the contact type, and 2) the experimentalist using a better strain gauge observes a change in the nonhomogeneous residual deformations in a standard tensile test if he also observes large-scale plastic strains. Coleman and Hodgdon (1985) and Zbib and Aifantis (1988) included gradients of the strain in the expression for the flow stress of the material and provided a different motivation for doing so, and did not consider higher order stresses in their works. In a series of papers Aifantis and co-workers (e.g. see Aifantis 1984; Vardoulakis and Aifantis 1991; and references cited therein), have motivated the consideration of higher-order deformation gradients in localization problems, and used these theories to compute widths of stationary shear bands in rigid plastic materials and the spacing of travelling Portevin-Le Chatelier bands in viscoplastic metals.

Each one of these approaches introduces a material characteristic length in addition to the viscous and thermal lengths. Batra and Kim (1991) have shown that, for the one-dimensional simple shearing problem, the band width tends to zero as the thermal length goes to zero for the Litonski and the Johnson-Cook flow rules. However, for the Bodner-Partom flow rule the band-width approached a finite value even when the thermal conductivity was reduced to zero. Since the materials considered by Batra and Kim were rate-dependent, their computed results suggest that, at least for the Litonski and the Johnson-Cook flow rules, the band width is not controlled by the viscous length. Here we investigate the dependence of solution variables upon the material characteristic length l.

The computed results indicate that the consideration of diploar effects stiffens the material repsonse in the sense that the rate of growth of the second invariant of the strain-rate tensor and temperature at the point of initiation of the shear band is lower as compared to that for nonpolar materials. Also, the width of the severely deforming region is more for diploar materials as compared to that for nonpolar materials.

2
Formulation of the problem

We use rectangular Cartesian coordinates to describe the dynamic thermomechanical deformations of an isotropic prismatic body of square cross-section being deformed in simple compression (cf. Fig. 1). We pressure that a plane strain state of deformation prevails. When second order gradients of the velocity field are also taken as independent kinematic variables and the corresponding higher-order (hereinafter referred to as dipolar) stresses as kinetic variables, equations governing the deformations of the body may be written as follows (e.g., see Mindlin (1965) who studies infinitesimal deformations of an elastic body).

$$\text{Balance of mass:} \quad v_{i,i} = 0, \tag{1}$$

$$\text{Balance of linear momentum:} \quad \rho \dot{v}_i = \sigma_{ij,j} - \tau_{ijk,jk}, \tag{2}$$

$$\text{Balance of internal energy:} \quad \rho \dot{e} = -q_{i,i} + \sigma_{ij} v_{i,j} + \tau_{ijk} v_{i,jk}. \tag{3}$$

These equations are written in the spatial description. In them, v denotes the velocity of a material particle, ρ the mass density, $\boldsymbol{\sigma}$ the Cauchy stress tensor, $\boldsymbol{\tau}$ the dipolar stress tensor, e the internal energy per unit mass, q the heat flux per unit area in the present configuration, a superimposed dot indicates the material time derivative, a comma followed by an index j indicates partial differentiation with

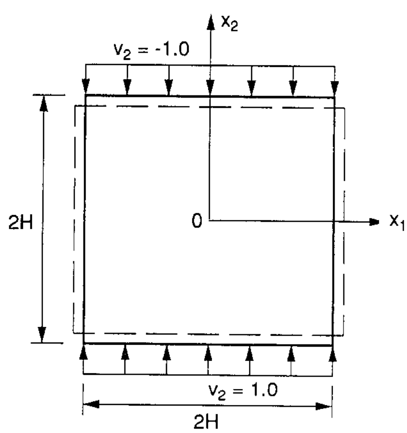

Fig. 1. A schematic sketch of the problem studied

respect to the present position x_j of a material particle, the usual summation convention is used, and ε_{ijk} is the permutation symbol that assumes the following values.

$$\varepsilon_{ijk}=\begin{cases}1, & \text{according as } i, j, k \text{ form an even permutation of 1, 2, and 3,}\\ -1, & \text{according as } i, j, k \text{ form an odd permutation of 1, 2, and 3,}\\ 0, & \text{if any two of the three indices are equal.}\end{cases} \tag{4}$$

We refer the reader to Mindlin (1965), Toupin (1962), Green et al. (1968), and Dillon and Kratochvil (1970) for motivation and derivation of these equations. Here we have followed an approach similar to that of Mindlin, and have assumed that the deformations of the body are isochoric, and the supplies of linear momentum and internal energy are null. Since our interest is in studying the intense plastic deformations of the body, we neglect its elastic deformations. We postulate that

$$\tau_{i[jk]}\equiv\tfrac{1}{2}(\tau_{ijk}-\tau_{ikj})=0, \tag{5}$$

and note that $\tau_{i[jk]}$ contributes nothing to the balance of linear momentum and the balance of internal energy. Green et al. (1968) made a similar assumption; our main reason for assuming (5) is to avoid finding constitutive relations for $\tau_{i[jk]}$ and keeping the formulation of the problem simple. A closer look at Eq. (2) reveals that $(\sigma_{ij}-\tau_{ijk,k})$ equals the flux of linear momentum.

In Eq. (3) we have assumed that all of the plastic work is converted into heat. Sulijoadikusumo and Dillon (1979) presumed that only about 90% of the plastic work was transformed into heat. Farren and Taylor (1925) found that in tensile experiments on steels, copper and aluminum, the heat rise represented 86.5, 90.5–92, and 95%, respectively, of the plastic work.

For the one-dimensional theory of dipolar materials, Wright and Batra (1987) provided some motivation for the assumption that the plastic strain-rate and plastic part of the dipolar strain-rate are proportional to the same plastic multiplier. Here we make a similar postulate, viz.,

$$D_{ij}\equiv\tfrac{1}{2}(v_{i,j}+v_{j,i})=\Lambda s_{ij}, \tag{6}$$

$$A_{ijk}=A_{ikj}=v_{i,jk}=\frac{\Lambda}{l^2}\tau_{ijk}, \tag{7}$$

where

$$s_{ij}=\sigma_{ij}+p\,\delta_{ij}, \tag{8}$$

p being the hydrostatic pressure not determined by the deformation of the body, and l is a material characteristic length. As in classical plasticity, we assume that a scalar yield or loading function f exists such that

$$f(s,\tau,\theta,D,A)=\kappa, \tag{9}$$

where κ describes the work hardening of the material. In (9), θ is the temperature rise of a material particle. We assume that plastic flow occurs for every value of s, τ, and θ, and find Λ from

$$f(s,\tau,\theta,\Lambda s,\Lambda\tau)=\kappa. \tag{10}$$

We restrict the loading function f to be such that the derivative f_Λ is negative for all values of other arguments. It ensures that Eq. (10) will have a unique solution with $\Lambda>0$. Motivated by the von Mises yield criterion in classical plasticity and the one-dimensional dipolar theory of Wright and Batra (1987), we select f and κ as follows.

$$f=\frac{s_e}{(1+b\Lambda s_e)^m(1-\alpha(\theta-\theta_0))}, \tag{11}$$

$$\kappa(\psi)=\sigma_0\left(1+\frac{\psi}{\psi_0}\right)^n, \tag{12}$$

$$\dot{\psi}=\frac{\Lambda s_e^2}{\sigma_0\left(1+\dfrac{\psi}{\psi_0}\right)^n}, \tag{13}$$

$$s_e^2 \equiv s_{ij}s_{ij} + \frac{1}{l^2}\tau_{i(jk)}\tau_{i(jk)}. \tag{14}$$

Here σ_0 is the yield stress of the material in a quasistatic simple tension or compression test, ψ_0 and n describe the work hardening of the material, b and m characterize its strain-rate hardening, α is the coefficient of thermal softening, and θ equals the present temperature of a material particle whose initial temperature was θ_0. The parameter ψ introduced through Eqs. (12) and (13) may be thought of as an internal variable and equated with the plastic strain. It describes the effect of the history of deformation on the current value of the yield stress. With κ interpreted as the axial stress and ψ the axial plastic strain, Eq. (12) describes the stress-strain curve for the material deformed quasistatically in simple tension or compression.

In addition to the foregoing, we need constitutive relations for the heat flux q and the specific internal energy e. For these, we take

$$q_i = -k\theta_{,i}, \tag{15}$$

$$e = c(\theta - \theta_0), \tag{16}$$

where c is the specific heat and k the thermal conductivity. Before stating the initial and boundary conditions we introduce nondimensional variables, indicated by a superimposed bar, as follows.

$$\bar{x} = x/H, \quad \bar{t} = t\dot{\gamma}_0, \quad \bar{v} = v/H\dot{\gamma}_0, \quad \bar{\kappa} = \kappa/\sigma_0, \quad \bar{\theta} = \theta/\theta_r, \quad \bar{s} = s/\sigma_0, \quad \bar{\tau} = \tau/l\sigma_0,$$

$$\bar{p} = p/\sigma_0, \quad \bar{\Lambda} = \Lambda\,\sigma_0/\dot{\gamma}_0, \quad \bar{s}_e = s_e/\sigma_0, \quad \bar{D} = D/\dot{\gamma}_0, \quad \bar{A} = A\,H/\dot{\gamma}_0,$$

$$\bar{l} = l/H, \quad \bar{\alpha} = \alpha\theta_r, \quad \bar{b} = b\dot{\gamma}_0, \quad \bar{k} = k/(\rho c\dot{\gamma}_0 H^2), \quad \bar{\rho} = \rho H^2\dot{\gamma}_0^2/\sigma_0, \tag{17}$$

where

$$\theta_r \equiv \sigma_0/\rho c, \quad \dot{\gamma}_0 \equiv v_0/H, \tag{18}$$

$2H$ is the length of a side of the square cross-section, and v_0 is the steady speed at which the top surface is compressed. Thus, $\dot{\gamma}_0$ equals the average strain-rate. Writing Eqs. (1) through (16) in terms of nondimensional variables and dropping the superimposed bars, we arrive at the following.

$$v_{i,i} = 0, \tag{19.1}$$

$$\rho\dot{v}_i = -p_{,i} + s_{ij,j} - l\tau_{ijk,jk}, \tag{19.2}$$

$$\dot{\theta} = k\theta_{,ii} + s_{ij}D_{ij} + l\tau_{ijk}A_{ijk}, \tag{19.3}$$

$$\dot{\psi} = \frac{s_{ij}D_{ij} + l\tau_{ijk}A_{ijk}}{\left(1 + \dfrac{\psi}{\psi_0}\right)^n}, \tag{19.4}$$

$$D_{ij} = \Lambda s_{ij}, \quad A_{ijk} = \frac{\Lambda}{l}\tau_{ijk}, \tag{19.5, 6}$$

$$s_e^2 = s_{ij}s_{ij} + \tau_{ijk}\tau_{ijk}, \tag{19.7}$$

$$\Lambda = \frac{I_e}{\left(1 + \dfrac{\psi}{\psi_0}\right)^n (1 - \alpha(\theta - \theta_0))(1 + bI_e)^m}, \tag{19.8}$$

$$I_e^2 \equiv D_{ij}D_{ij} + l^2 A_{ijk}A_{ijk}. \tag{19.9}$$

Equations (19.2), (19.3), (19.4), (19.8), and (19.9) reduce to those for simple (nonpolar) materials when l is set equal to zero in them. These equations with l set equal to zero and subject to suitable initial and boundary conditions have been studied extensively by Batra and Liu (1989), Batra and Zhu (1991), and Batra and Zhang (1990) as far as the initiation and growth of a shear band at an inhomogeneity is concerned.

We presume that the initial values of θ and ψ are symmetric and those of v_1 and v_2 are antisymmetric in x_1 and x_2, and seek solutions of Eqs. (19.1) through (19.9) with the same symmetries. Thus, the problem is to be studied over the spatial domain $[0, b] \times [0, h]$ and the boundary conditions become

$$v_1(0, x_2, t) = 0, \quad \theta_{,1}(0, x_2, t) = 0, \quad (\sigma_{21} - l\tau_{21k,k})|_{(0,x_2,t)} = 0, \tag{20.1}$$

$$v_2(x_1, 0, t) = 0, \quad \theta_{,2}(x_1, 0, t) = 0, \quad (\sigma_{12} - l\tau_{12k,k})|_{(x_1,0,t)} = 0, \tag{20.2}$$

$$v_2(x_1, h, t) = -1, \quad \theta_{,2}(x_1, h, t) = 0, \quad (\sigma_{12} - l\tau_{12k,k})|_{(x_1,h,t)} = 0, \tag{20.3}$$

$$\theta_{,2}(b, x_2, t) = 0, \quad (\sigma_{i1} - l\tau_{i1k,k})|_{(b,x_2,t)} = 0. \tag{20.4}$$

For the initial conditions, we take

$$v_1(x_1, x_2, 0) = x_1, \quad v_2(x_1, x_2, 0) = -x_2, \tag{21.1}$$

$$\begin{aligned}\theta(x_1, x_2, 0) &= \theta_0 + \varepsilon(1 - r^2)^9 e^{-5r^2}, \quad r^2 = x_1^2 + x_2^2, \quad r \leqq 1,\\ &= \theta_0, \quad r > 1.\end{aligned} \tag{21.2}$$

Here b and h equal, in the present configuration, the length of the base and the height of the quarter of block. The boundary conditions (20) imply that the boundaries of the block are thermally insulated, the right surface is free of flux of linear momentum, there is no flux of linear momentum in the tangential direction on the other three bounding surfaces, and the normal component of velocity on the left and bottom surfaces vanishes. The boundary conditions on the left and bottom surfaces follow from the assumed symmetry of the deformation field. The initial conditions on the velocity field represent the situation when the transients have just died out. It is highly unlikely that the transients will die out at the same instant throughout the body. However, the assumption is justified on the grounds that it reduces significantly the CPU effort required to solve the problem and does not affect the qualitative nature of computed results. The initial temperature distribution given by (21.2) models a material inhomogeneity; the amplitude ε of the perturbation can be thought of as representing the strength of the singularity.

One way to motivate the aforestated mechanical boundary conditions is to take the inner product of Eq. (19.2) with a smooth virtual displacement, integrate the resulting equation over the domain occupied by the body at time t, and use the divergence theorem. The term involving integration on the boundary of the domain suggests mechanical boundary conditions stated in Eq. (20).

The initial-boundary-value problem defined by Eqs. (19) through (21) is highly nonlinear. There is no hope of proving an existence or uniqueness theorem for it. Here we seek its approximate solution by the finite element method.

3
Computational considerations

Since second order spatial derivatives of the dipolar stress $\underset{\sim}{\tau}$ appear in the balance of linear momentum (19.2), we introduce auxiliary variables f by

$$f_{ij} = \tau_{ijk,k}. \tag{22}$$

We use the Galerkin approximation (e.g., see Hughes 1987) to derive the weak form of Eqs. (19) and (22). The natural boundary conditions $(20.1)_{2,3}$, $(20.2)_{2,3}$, $(20.3)_{2,3}$, and (20.4) are incorporated into the weak formulation of the problem obtained by using the Galerkin approximation. The auxiliary variables f are eliminated at the element level, and nodal values of s and τ are expressed in terms of the nodal values of $\boldsymbol{D}$ and $\boldsymbol{A}$ by using Eqs. (19.5) and (19.6). By using Eq. $(6)_1$ and the intermediate variable $g_{ij} \equiv v_{i,j}$, we express the nodal values of $\boldsymbol{D}$ and $\boldsymbol{A}$ in terms of the nodal values of $\boldsymbol{v}$. The reason for introducing auxiliary or intermediate variables is to have, at most, first order derivatives of various field quantities. It enables us to select test functions and trial solutions from the space H^1 of functions, which includes functions defined on the domain of interest and whose first order derivatives are square integrable. The disadvantage of having auxiliary and/or intermediate variables is that the number of unknowns becomes very large. It is obviated somewhat herein by eliminating these auxiliary variables before integrating the ordinary differential equations with respect to time t. Here we use four-noded quadrilateral elements and regard the pressure to be constant within each element. We employ 2×2 Gauss quadrature rule to evaluate various integrals over an element. The result of this exercise is a set of coupled highly nonlinear ordinary differential equations (ODEs) for the nodal values of the two components of the velocity, temperature, and the internal variable ψ, and a set of algebraic equations for values of the hydrostatic pressure at the element centroids. Thus, the number of ODEs equals four times the number of nodes, and the number of algebraic equations equals the number of elements in the mesh.

In deriving the above-referenced ODEs, a lumped mass matrix obtained by using the special lumping technique (e.g., see Hughes 1987) is employed. Even though there is no mathematical theory to support it, the lumped mass matrix so obtained gives optimal rates of convergence and works well for structural and solid mechanics problems (Hinton et al. 1976).

The ODEs are integrated with respect to time t by using the trapezoidal rule (Hughes 1987), which is a member of the Newmark family of methods. For linear problems, the method is implicit, second order accurate, and unconditionally stable. For the nonlinear problem studied herein, the time step had to be controlled to achieve stability. The application of the trapezoidal rule results in a system of coupled nonlinear algebraic equations, which are solved iteratively for the nodal values of the two components of the velocity $\boldsymbol{v}$, temperature θ, and the internal variable ψ and values of p at the element centroids. The iterative process is stopped when, at each node point, either

$$\frac{|\Delta v_1|}{|v_1|}+\frac{|\Delta v_2|}{|v_2|}+\frac{|\Delta \theta|}{\theta}+\frac{|\Delta \psi|}{\psi} \leqq \varepsilon_1, \quad \text{or} \tag{23.1}$$

$$|\Delta v_1|+|\Delta v_2|+|\Delta \theta|+|\Delta \psi| \leqq \varepsilon_2, \tag{23.2}$$

where ε_1 and ε_2 are preassigned small numbers, and $\Delta\theta$ denotes the differences in the nodal values of θ during two successive iterations within the same time increment. A reason for applying either criterion (23.1) or (23.2) is that, at nodes on the boundary where essential boundary conditions are prescribed to be zero, criterion (23.1) is meaningless.

A few trial runs indicated that $\Delta t = 5 \times 10^{-5}$ was a good starting step size. The time step size was reduced by a factor of 0.7 chosen by trial and error, every time the convergence criterion (23.1) or (23.2) failed. In a typical run, Δt had to be reduced ten times so that, during the final stages of computation, Δt equalled 0.1412×10^{-5}.

4
Computation and discussion of results

We took the following values of various material and geometric parameters to compute numerical results.

$$b = 10000\,\text{sec}, \quad \alpha = 0.0222\,{}^\circ\text{C}^{-1}, \quad \sigma_0 = 333\,\text{MPa}, \quad k = 49.22\,\text{Wm}^{-1}\,{}^\circ\text{C}^{-1},$$

$$c = 473\,\text{Jkg}^{-1}\,{}^\circ\text{C}^{-1}, \quad \rho = 7860\,\text{kg}\,\text{m}^{-3}, \quad m = 0.025, \quad n = 0.09,$$

$$\psi_0 = 0.017, \quad H = 5\,\text{mm}, \quad \dot{\gamma}_0 = 5000\,\text{sec}^{-1}, \quad \varepsilon = 0.2,$$

$$\varepsilon_1 = 10^{-3}, \quad \varepsilon_2 = 10^{-3}, \quad \theta_0 = 0. \tag{24}$$

These values, except that for the coefficient of thermal softening, are for a typical steel and were used by Batra and Liu (1989) and Batra and Ko (1992). They studied the problem for nonpolar materials only. Whereas Batra and Liu used nine-noded quadrilateral elements, Batra and Ko used an adaptively refined mesh consisting of three-noded triangular elements to study the problem. Both these studies considered volumetric elastic strains and assumed the material to be compressible. The purposely chosen high values of the thermal softening coefficient and the magnitude of the initial temperature perturbation should reduce significantly the computational time required to analyze the problem. It should not affect the qualitative nature of results reported herein. For the values given above, $\theta_r = 89.6\,{}^\circ$C, and the nondimensional melting temperature equals 0.5027. We note that the test data to find values of material parameters at strains, strain-rates, and temperatures likely to occur in a shear band is not available in the open literature. It is also not clear to what material variables like the grain size, mean distance among dislocations, etc. is the material characteristic length l related. Therefore, we study the problem for a range of values of l.

Figure 2 depicts the vertical load and the effective stress s_e versus the average strain in the vertical direction when the block is deformed homogeneously, i.e., with no temperature perturbation introduced initially and the material characteristic length l set equal to zero. The vertical load P on the top surface is given by

$$P = -\int_0^1 (\sigma_{22}(x_1, h, t) - l\tau_{222,2}(x_1, h, t))\, dx_1 \tag{25}$$

where the negative sign in front of the integral is to get a positive value of P. For homogeneous deformations of the block, the dipolar stress vanishes identically. In order to evaluate P, we need to find the value of the hydrostatic pressure p at points on the top surface. Since p is assumed to be constant within each element, its values at the node points are computed by using the following smoothing technique.

$$\sum_\beta \left(\int_\Omega \Phi_\alpha \Phi_\beta \, d\Omega \right) p_\beta = \sum_e \int_{\Omega_e} \Phi_\alpha p \, d\Omega. \tag{26}$$

Here $\{\phi_\alpha, \alpha = 1, 2, \ldots\}$ is the set of piecewise linear finite element basis functions defined on Ω, $p_1, p_2, \ldots$ are nodal values of the hydrostatic pressure, and p on the right hand side of Eq. (26) is the piecewise constant pressure field computed as a solution of the problem. It is obvious from the plot of Fig. 2 that the peak in the load occurs at an average strain of 0.012, and beyond this value of the average strain, the softening caused by the heating of the material exceeds the hardening due to the strain and strain-rate effects. The difference between the magnitude of the vertical load and the effective stress is due to the hydrostatic pressure. Note that our definition of the effective stress differs from the usual one by a constant factor.

In Fig. 3, we have plotted the vertical load versus the average strain curves for $l = 0$, 0.05, and 0.1 when there is a temperature perturbation introduced. Thus, the deformations of the block will be

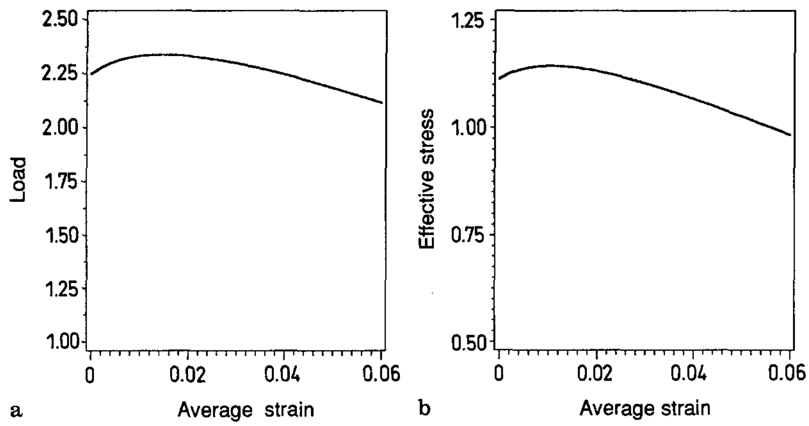

Fig. 2. Vertical load and effective stress versus the average strain in the vertical direction for homogeneous deformations of the block

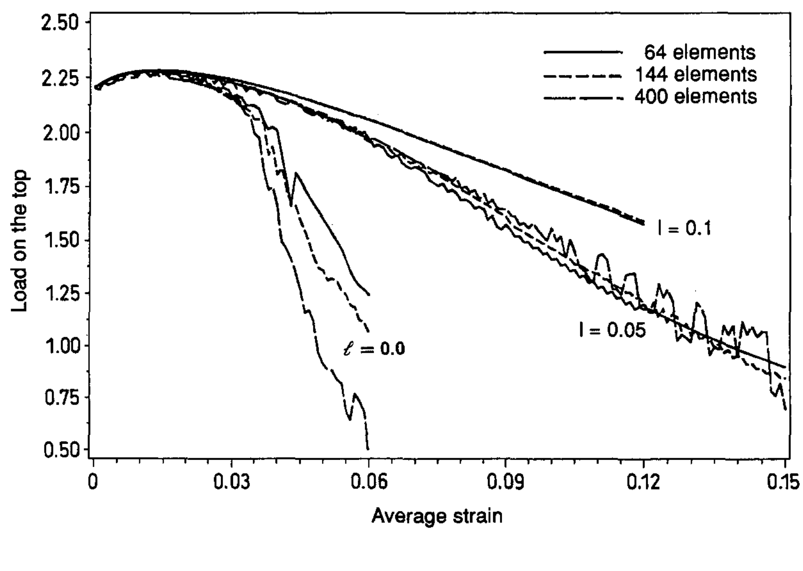

Fig. 3. Vertical load versus the average strain in the vertical direction for $l = 0$, 0.05, and 0.1, and three different finite element meshes of 64, 144 and 400 uniform elements in the reference configuration

nonuniform. The results were computed with three initial meshes having eight, twelve, or twenty uniform elements in both the horizontal and vertical directions. The coordinates of the node points are updated after each time increment so that once the block begins to deform nonhomogeneously, the finite element mesh becomes nonuniform. The plotted results reveal that, for nonpolar materials with $l = 0.0$, the load drops severely soon after its peak occurs. At an average strain of 0.06, the load has dropped to nearly half of its peak value for the 64-element mesh and to 22% of the peak value for the 400-element mesh. The results computed with the 144-element and 400-element meshes are smoother and the drop in the load is more than that obtained by using the 64-element mesh. For $l = 0.05$ and $l = 0.1$, the drop in the load is less rapid and the rate of drop in load with increasing average strain decreases with an increase in the value of l. Also, the dependence of the computed value of the load upon the mesh used decreases with an

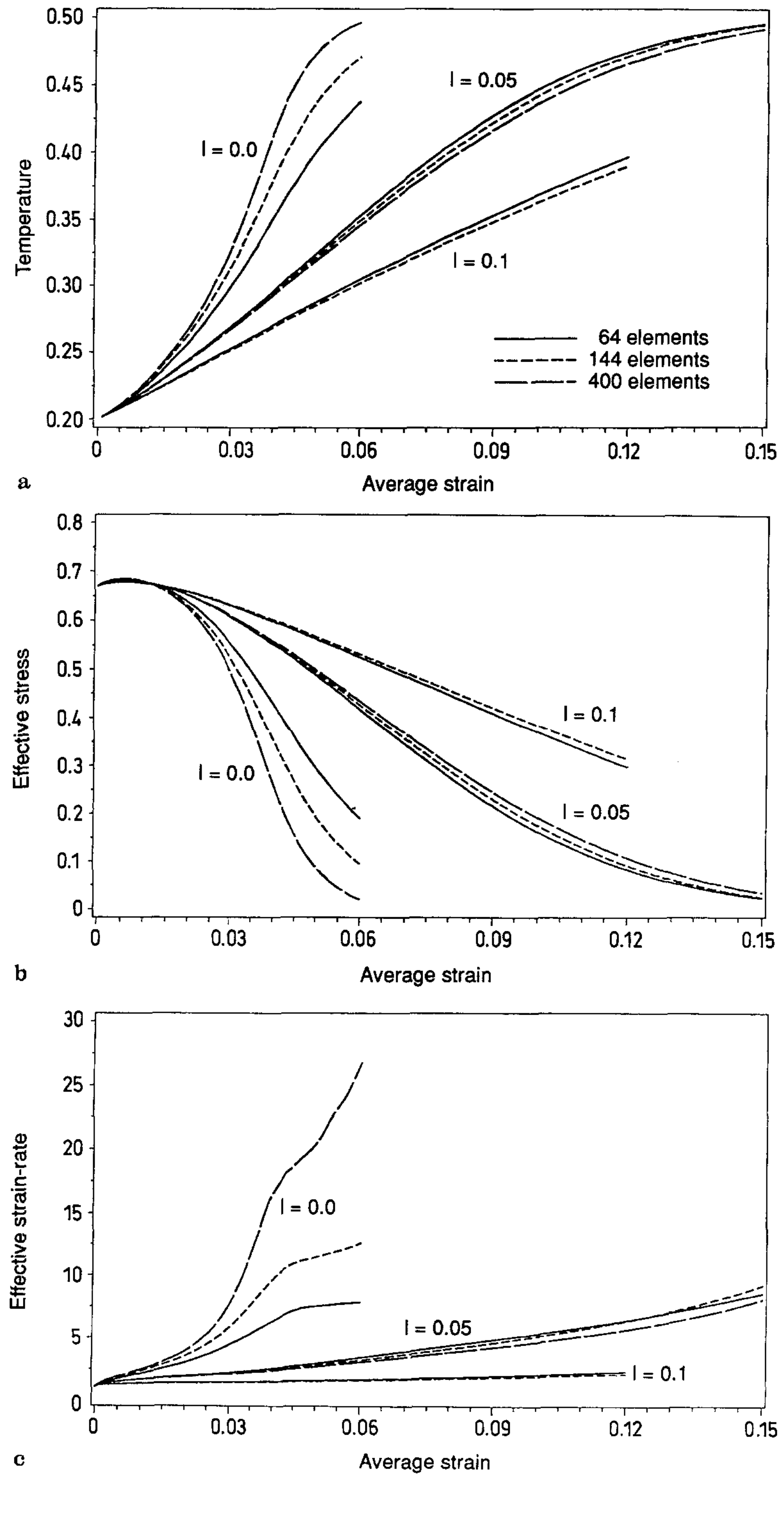

Fig. 4. The evolution of the temperature, effective stress, and the effective strain-rate at the block center for three different meshes and three different values of l

increase in the value of l, the results for the three meshes used being essentially identical for $l = 0.1$. At an average strain of 0.06 and for the 144 element mesh, the vertical load has dropped to 1.06, 2.0 and 2.05 from a peak of 2.275 for $l = 0.0$, 0.05, and 0.1, respectively.

The evolution of the temperature, effective stress s_e, and effective strain-rate I_e at the block center where the applied temperature perturbation takes on its highest value are depicted in Figs. 4a–c, respectively. The nondimensional effective stress and effective strain-rate are defined by Eqs. (19.7) and (19.9), respectively. The evolution of the effective stress at the block center is similar to that of the applied load in the sense that it first increases and then decreases with an increase in the average strain in the specimen. However, because of the temperature perturbation applied at the block center, the peak in the effective stress occurs at a much lower value of the average strain as compared to that at which the applied load attains it maximum value in Fig. 2. The finer meshes of 144 and 400 elements give sharper results than those obtained with 64 elements in the sense that the effective strain-rate increases more rapidly, the temperature rise is more, and the drop in the effective stress is more

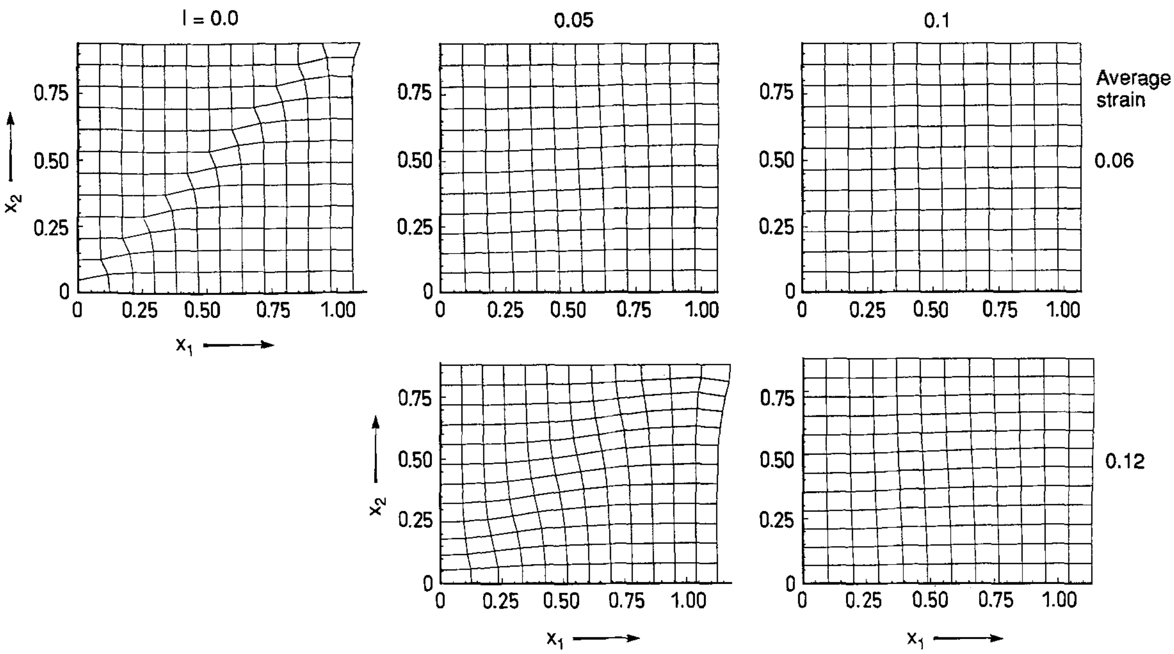

Fig. 5. The deformed meshes at an average strain of 0.06 and three different values of l, and at an average strain of 0.12 for $l = 0.05$ and 0.1

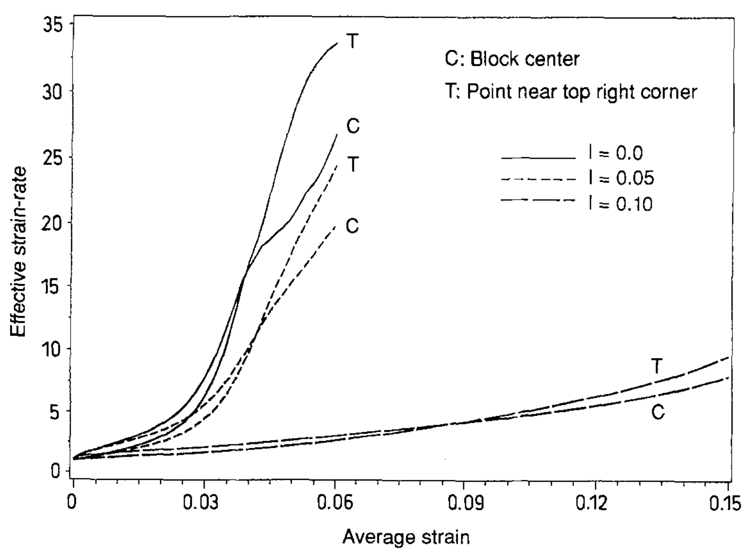

Fig. 6. Evolution of the effective strain-rate at the block center and at a point near the top right corner for nonpolar and dipolar materials

severe. For $l = 0.05$ and 0.1, the differences in the solution variables obtained with different meshes become minuscule enough to conclude that the results are independent of the mesh used for $l = 0.1$. The consideration of dipolar effects does not alter the qualitative nature of computed resuts, except that the temperature rise, the drop in the effective stress, and the evolution of the effective strain-rate at

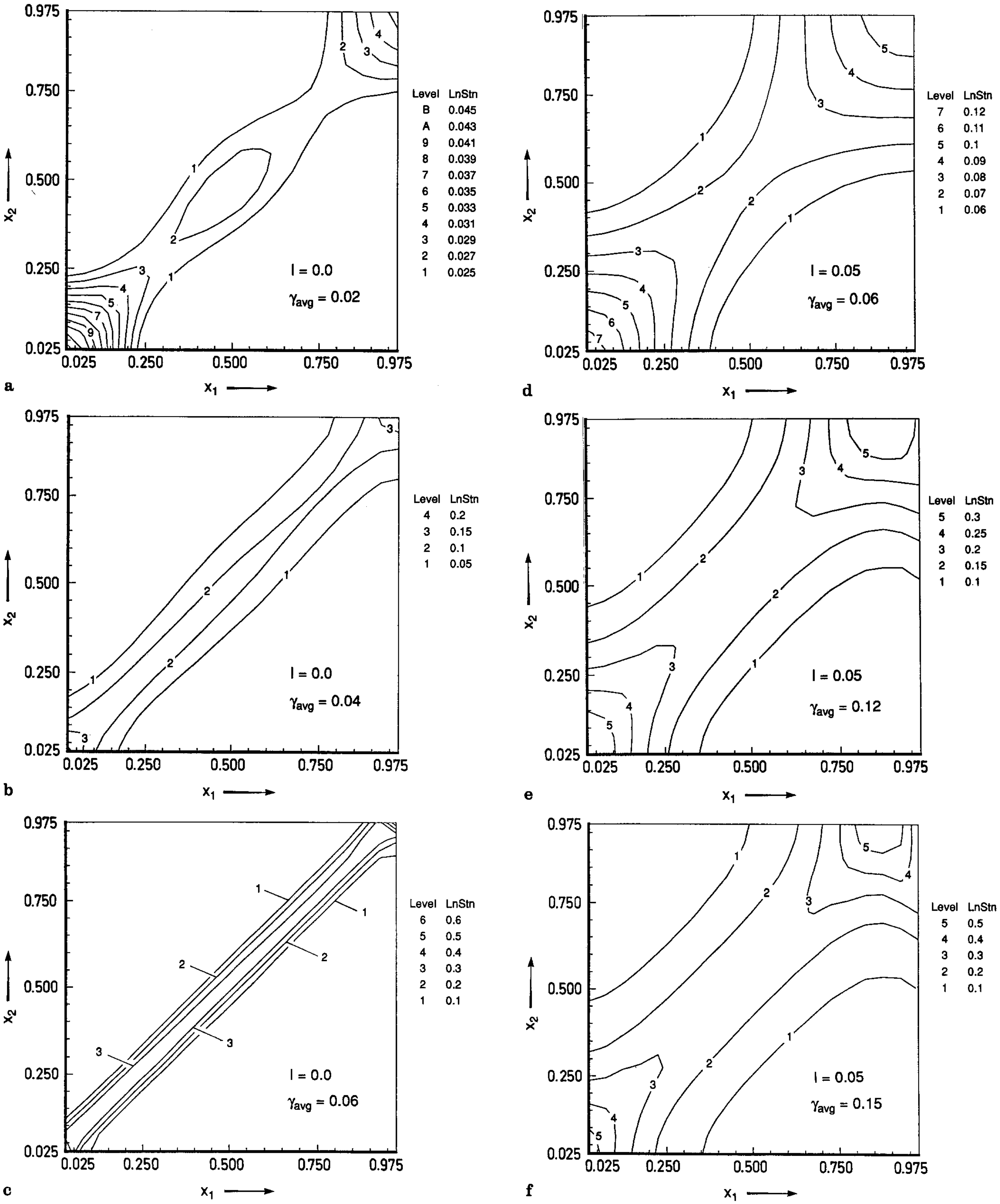

Fig. 7. Contours, in the reference configuration, of the maximum principal logarithmic strain for nonpolar materials at $\gamma_{avg} = 0.02$, 0.04, and 0.06, and for dipolar materials with $l = 0.05$ at $\gamma_{avg} = 0.06$, 0.12, and 0.15

the block center for a fixed value of the average strain are higher for nonpolar materials than that for dipolar materials.

In order to see how the elements are distorted, we have plotted in Fig. 5 the deformed meshes at an average strain, γ_{avg}, of 0.06 for $l = 0$, 0.05, and 0.1, and the deformed meshes at an average strain of 0.12 for $l = 0.05$ and 0.1. It is clear that, for $l = 0$ and $\gamma_{avg} = 0.06$, elements along the main diagonal passing through the block center are severely distorted, and the straining of the elements is far less for dipolar materials with $l = 0.05$ as compared to that for nonpolar materials. For $l = 0.1$, the elements seem not to be distorted at all. At an average strain of 0.12, the elements along the main diagonal have undergone intense deformations for $l = 0.05$, but the body is deformed essentially homogeneously for $l = 0.1$. Since the tangential flux of linear momentum at the top surface is assumed to be zero, the material points there slide to the right as the block is compressed. For low values of l, this results in significant deformations of the element adjoining the top right corner, and the effective strain-rate there eventually exceeds that at the block center. It is shown in Fig. 6 for a 12 × 12 uniform mesh. We note that Batra and Ko (1993) obtained similar results for the axisymmetric compression of the block. This observation suggests that the singularity in the deformations caused by the difference in the boundary conditions on the two surfaces that meet at the top right corner may be enough to cause the initiation of the severe deformations and, hence, of the localization of the deformation. That this is not so is confirmed by the results computed without introducing a temperature perturbation at the block center. In this case, the deformations of the block stayed essentially uniform.

The computation of results for different values of the material characteristic length l revealed that the CPU time needed to study the problem for a fixed mesh increased significantly with an increase in the value of l, and for a fixed value of l, the CPU time increased with a refinement of the mesh. In order to conserve on the available computational resources and still use a reasonably fine mesh, we subsequently used a 20 × 20 uniform mesh and computed results for $l = 0$, 0.01, and 0.05. Figure 7 depicts contours in the reference configuration of the maximum

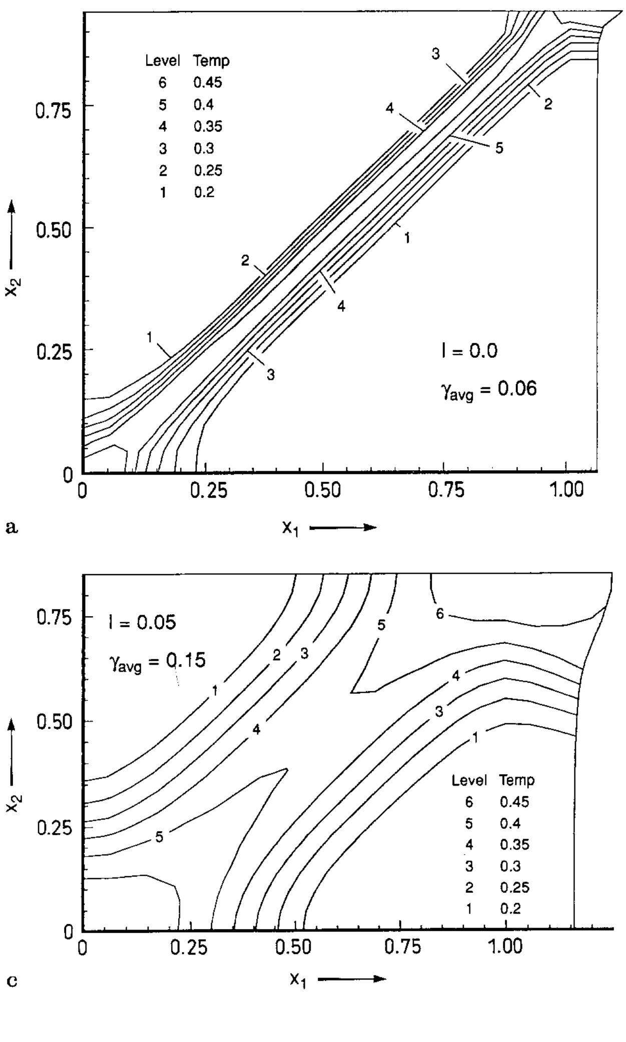

Fig. 8. Contours, in the present configuration, of the temperature rise for nonpolar and dipolar materials with $l = 0.01$ at $\gamma_{avg} = 0.06$, and for dipolar materials with $l = 0.05$ at $\gamma_{avg} = 0.15$

principal logarithmic strain ε_p, defined as

$$\varepsilon_p = \ln \lambda_1 = -\ln \lambda_2 \tag{27}$$

at the average strain $\gamma_{avg} = 0.02$, 0.04, and 0.06 and for $l = 0.0$ and at $\gamma_{avg} = 0.06$, 0.12 and 0.15 for $l = 0.05$. Here λ_1^2, λ_2^2, and 1 equal eigenvalues of the left Cauchy-Green tensor or the right Cauchy-Green tensor and the equality $(27)_2$ follows from the assumption that the deformations are isochoric. These plots suggest that contours of successively higher values of ε_p originate at the block center and propagate outward along the main diagonal. As the block continues to be compressed, the severely deforming region narrows down and eventually forms a thin band. For nonpolar materials, peak values of ε_p at $\gamma_{avg} = 0.02$, 0.04, and 0.06 were found to be 0.049, 0.217, and 0.684, respectively. The corresponding values for diploar materials with $l = 0.01$ equalled 0.046, 0.164, and 0.436, respectively. At $\gamma_{avg} = 0.06$, the contour of $\varepsilon_p = 0.3$ has traversed all along the main diagonal for nonpolar materials, but for dipolar materials with $l = 0.05$ the contour of $\varepsilon_p = 0.3$ has not even initiated. This verifies the assertion made above that, at the same value of the average strain, the elements along the main diagonal are deformed less severely for dipolar materials as compared to that for nonpolar materials. 365

At an average strain of 0.06, we have plotted in Fig. 8 contours of the temperature rise θ in the present configuration for nonpolar and diploar materials with $l = 0.01$. Also depicted are contours of θ when $\gamma_{avg} = 0.15$ and the material is dipolar with $l = 0.05$. For nonpolar materials, the contour of $\theta = 0.4$ has propagated along the main diagonal. But for dipolar materials with $l = 0.01$ it has moved away from the corners only a little bit. When $l = 0.05$, the contour of $\theta = 0.4$ propagates inwards from the centroid and the top right corner but has not moved all along the main diagonal even when $\gamma_{avg} = 0.15$. This is to be expected since elements along the main diagonal are deformed more intensely for nonpolar materials than for dipolar materials. The distribution of v_1 and v_2 within the domain at $\gamma_{avg} = 0.06$ for $l = 0$ and 0.01, and at $\gamma_{avg} = 0.15$ for $l = 0.05$ plotted in Fig. 9, wherein the distribution of only v_2 is shown, indicates that the deforming region is divided into two parts essentially separated along the diagonal passing through the block center. Each region is moving as a rigid body with all of the deformations concentrated in the narrow region separating the two parts. The plotted velocity field supports the assertion made by Massey (1921) that the tangential velocity field is discontinuous across the shear band. In our computations, the velocity field is assumed to be continuous. However, the sharp jumps in the values of v_1 and v_2 across the narrow region lend credence to Massey's proposal.

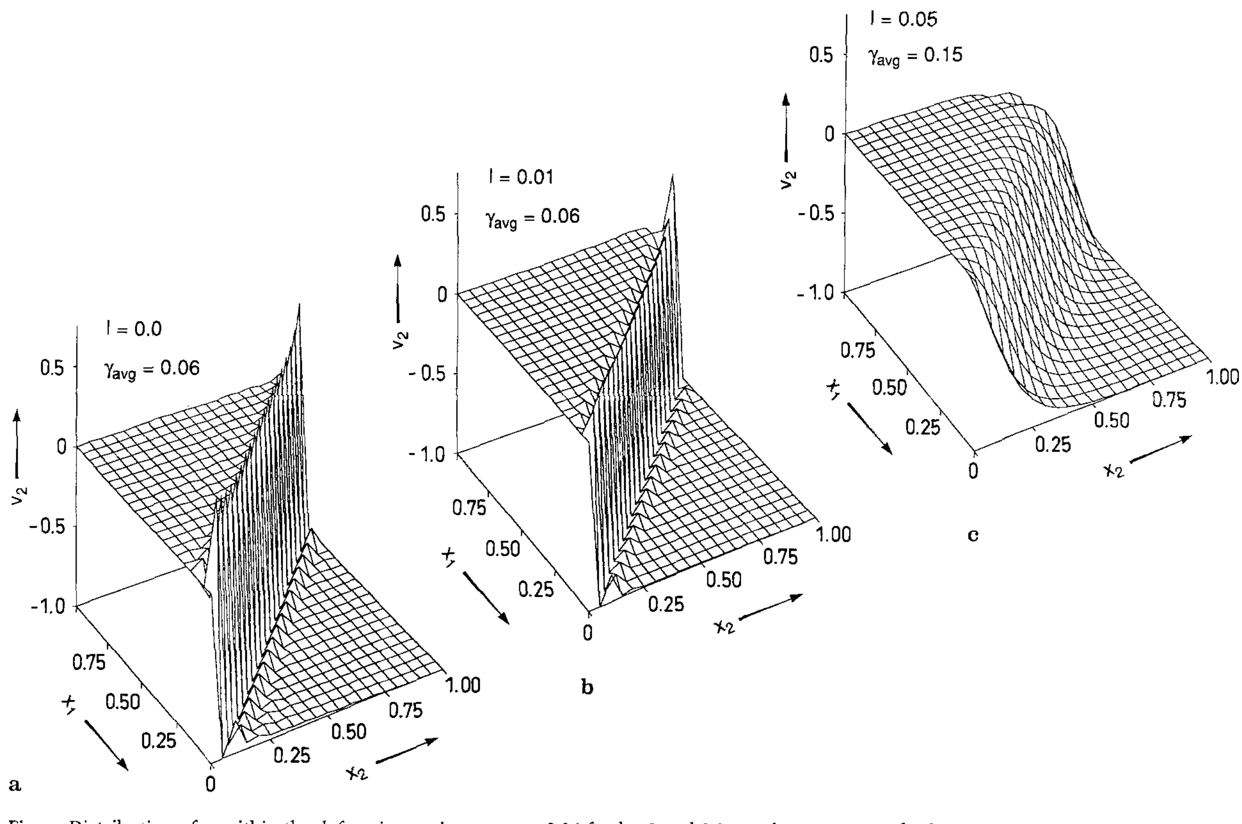

Fig. 9. Distribution of v_2 within the deforming region at $\gamma_{avg} = 0.06$ for $l = 0$ and 0.01, and at $\gamma_{avg} = 0.15$ for $l = 0.05$

Figure 10 depicts the contours of the effective dipolar stress τ_e, defined as

$$\tau_e^2 = \tau_{ijk}\,\tau_{ijk}$$

at an average strain of 0.12 for a 144 element mesh and for $l = 0.05$ and 0.10. These contours evince that the maximum value of τ_e occurs not at the band center, but at points far away from it. The magnitude of the peak value of τ_e and its location depend upon the value of l. These results are in qualitative agreement with those computed by Batra (1987) and by Batra and Kim (1988) for the one-dimensional problem.

From contours of the maximum principal logarithmic strain and the temperature rise, one can estimate the centerline EF of the shear band. In Fig. 11 we have shown how the effective strain-rate and the temperature rise vary along EF for nonpolar and dipolar materials with $l = 0.01$ at $\gamma_{avg} = 0.06$ and for dipolar materials with $l = 0.05$ at $\gamma_{avg} = 0.15$. Each quantity has been normalized with respect to its peak value on line EF. Both for nonpolar and dipolar materials the temperature rise is essentially concentrated near the block center and the top right corner. In these regions, material points are deforming more severely than those on the remainder of line EF. The effective stress varies more smoothly along the centerline EF for dipolar materials as compared to that for nonpolar materials. Figure 12 depicts the variation of the effective stress, effective strain-rate, and temperature rise on two lines AB and CD perpendicular to EF; the location of these lines is also shown in the figure. The various quantities have been normalized with respect to their maximum values on AB and CD. The plots of the distribution of the effective strain-rate and the temperature rise suggest that wider bands form for dipolar materials as compared to that for nonpolar materials. The difference between the bandwidth for nonpolar and diplar materials increases with an increase in the value of the material characteristic length l. Batra and Kim

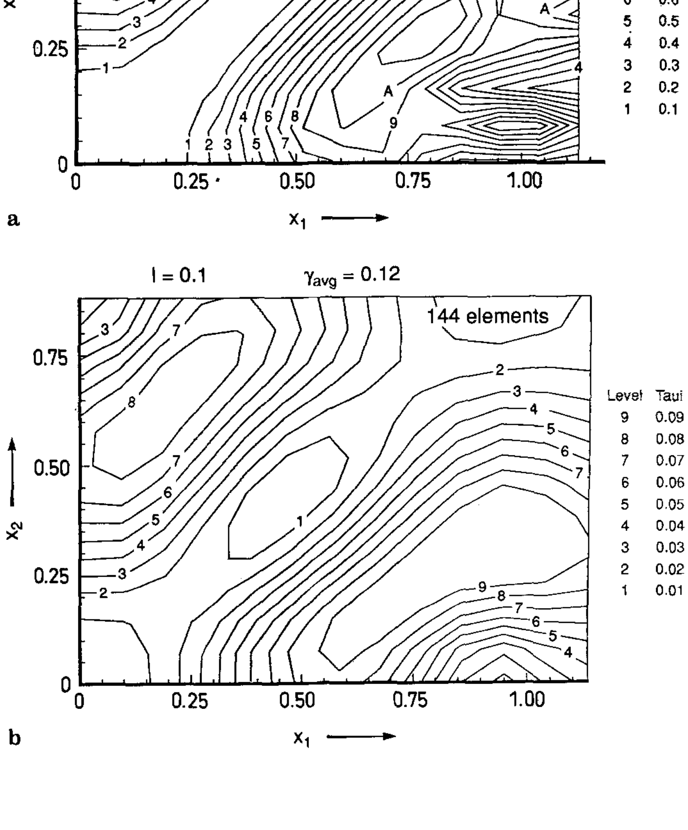

Fig. 10. Contours at $\gamma_{avg} = 0.12$ of the effective diploar stress for $l = 0.05$ and 0.10 for the 144 element mesh

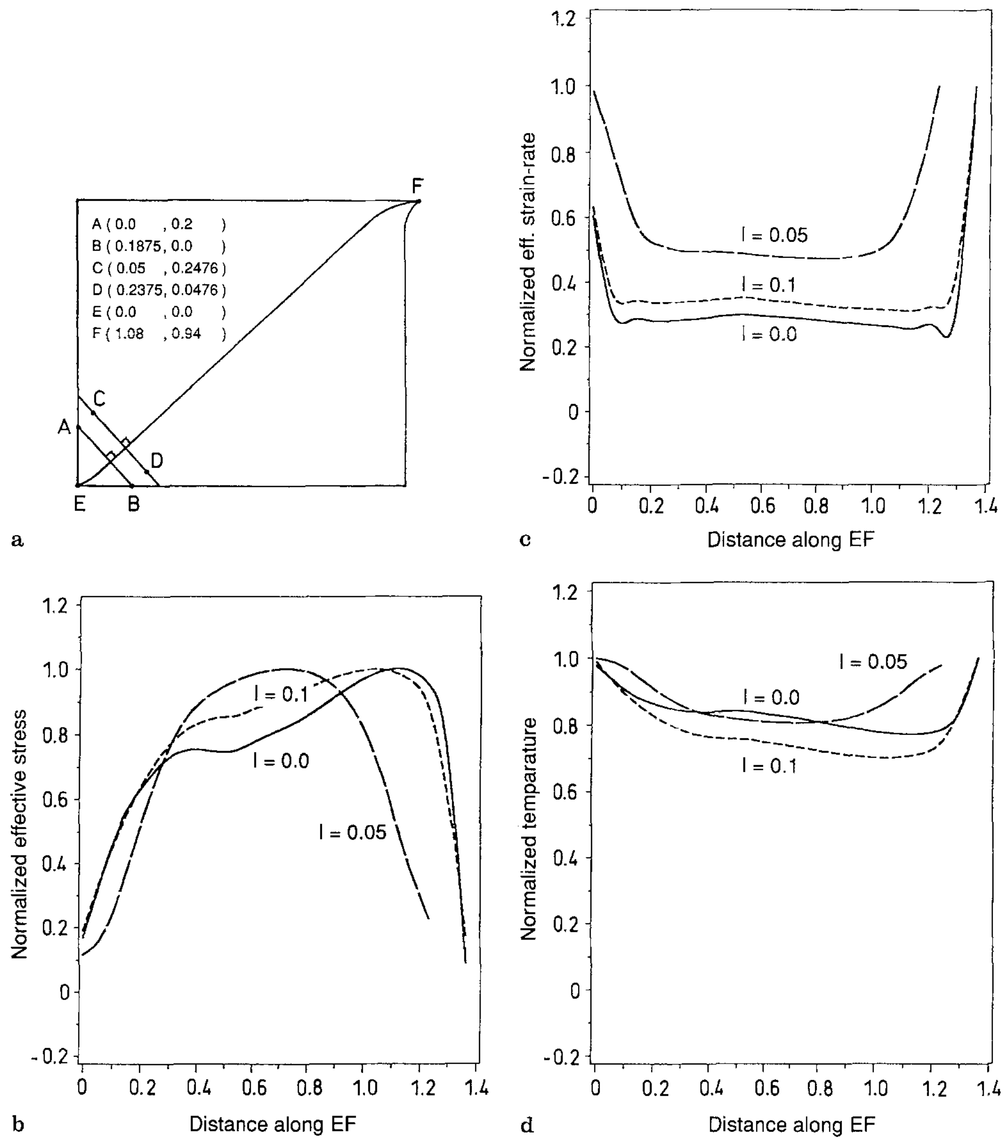

Fig. 11a–d. a Location of the band centerline EF, and of lines AB and CD perpendicular to EF. b–d Variation along the band centerline EF of the effective stress, effective strain-rate and the temperature rise for nonpolar and dipolar materials with $l = 0.01$ at $\gamma_{avg} = 0.06$, and for diploar materials with $l = 0.05$ at $\gamma_{avg} = 0.15$

(1988) studied the one-dimensional shear band problem and also concluded that the band width increased with an increase in the value of the material characteristic length l.

5
Conclusions

We have studied the initiation and growth of a shear band in a dipolar thermally softening viscoplastic body deformed in plane strain compression at a nominal strain-rate of 5000 sec^{-1}. Simple constitutive relations have been proposed for dipolar stresses. The proposed theory generalizes to three-dimensions the one-dimensional theory of Wright and Batra (1987) for dipolar materials, and the three-dimensional theory of Green et al. (1968) for rate-independent perfectly plastic materials to rate-dependent strain hardening but thermally softening dipolar materials. A finite element code capable of solving an initial-boundary-value problem involving plane strain deformations of these materials has been developed. It is shown that a shear band initiates from the block center where an initial temperature perturbation is introduced and propagates along the main diagonal. The consideration of dipolar effects has a stiffening effect in the sense that the initiation of the band is delayed and the rate of growth of the temperature and effective strain-rate at the band center is lower than that for nonpolar materials. These effects are enhanced by an increase in the value of the material characteristic length for the material. Also, the band is wider for dipolar materials as compared to that for nonpolar materials.

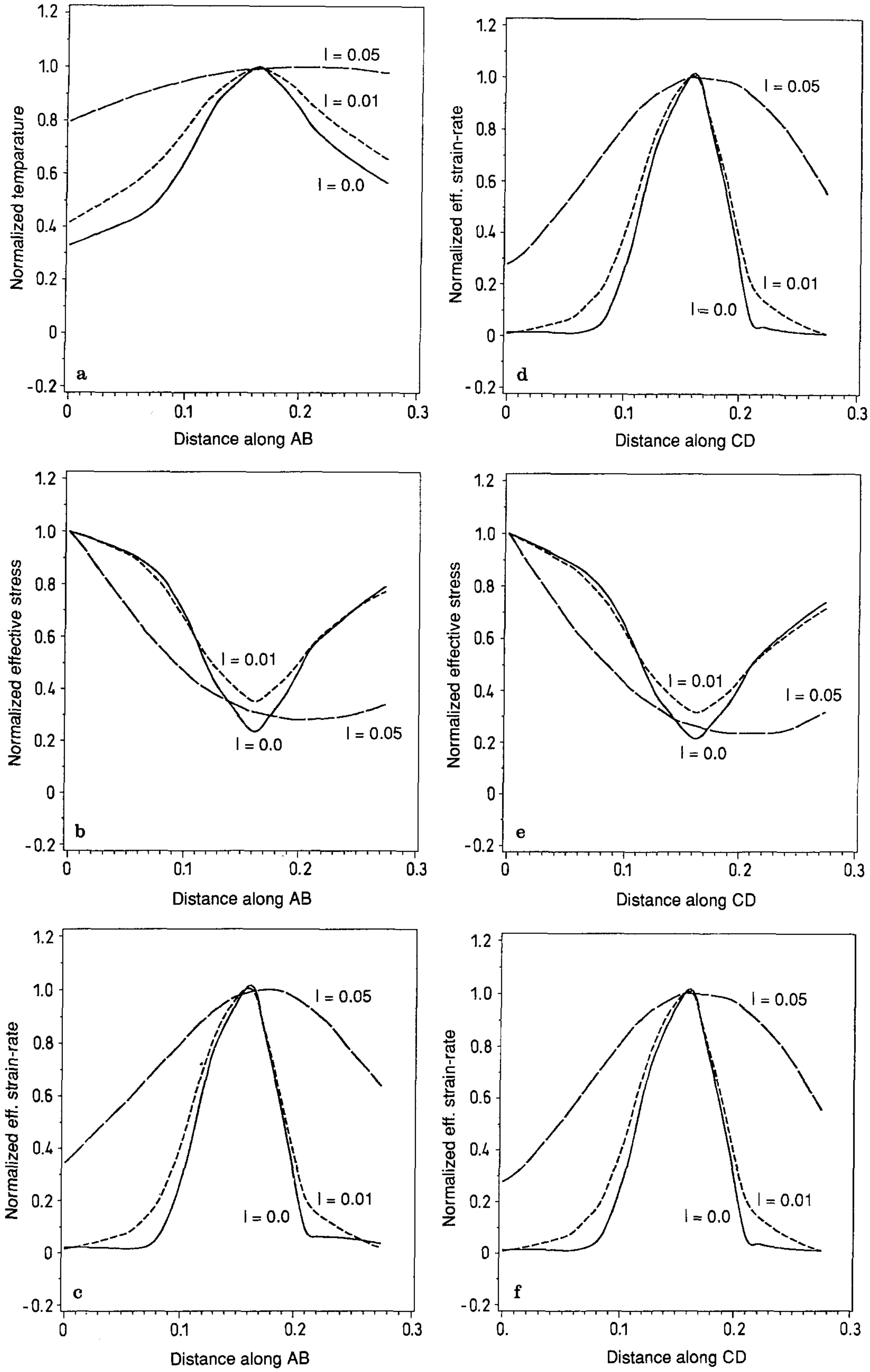

Fig. 12. Variation along lines AB and CD of the effective stress, effective strain-rate, and the temperature rise for nonpolar and dipolar materials with $l = 0.01$ at $\gamma_{avg} = 0.06$, and for dipolar materials with $l = 0.05$ at $\gamma_{avg} = 0.15$. Lines AB and CD are perpendicular to the band centerline

References

Aifantis, E. C. 1984: On the microstructural origin of certain inelastic models. J. Engr. Mat. Tech. 106: 326–330

Bai, Y.; Dodd, B. 1992: Adiabatic shear localization. Occurrence, theories and applications. Pergamon Press, New York

Batra, R. C. 1987: The initiation and growth of, and the interaction among, adiabatic shear bands in simple and dipolar materials. Int. J. Plasticity 3: 75–89

Batra, R. C.; Kim, C. H. 1988: Effect of material characteristic length on the initiation, growth and bandwidth of adiabatic shear bands in dipolar materials. J. de Physique 49(C3): 41–46

Batra, R. C.; Liu, De-Shin 1989: Adiabatic shear banding in plane strain problems. Arch. Rat'l Mechs. Anal. 56: 527–534

Batra, R. C.; Zhang, X. T. 1990: Shear band development in dynamic loading of a viscoplastic cylinder containing two voids. Acta Mechanica 85: 221–234

Batra, R. C.; Kim, C. H. 1991: Effect of thermal conductivity on the initiation, growth, and bandwidth of adiabatic shear bands. Int. J. Engr. Sci. 29: 949–960

Batra, R. C.; Zhu, Z. G. 1991: Dynamic adiabatic shear band development in a bimetallic body containing a void. Int. J. Solids and Structures 27: 1829–1854

Batra, R. C. 1992: Analysis of shear bands in simple shearing deformations of nonpolar and dipolar materials. Applied Mechs. Reviews 45, No. 3(2): S123–S131

Batra, R. C.; Ko, K. I. 1992: An adaptive mesh refinement technique for the analysis of shear bands in plane strain compression of a thermoviscoplastic solid. Computational Mechs. 10: 369–379

Batra, R. C.; Ko, K. I. 1993: Analysis of shear bands in dynamic axisymmetric compression of a thermoviscoplastic cylinder. Int. J. Engng. Sci. 31: 529–547

Coleman, B. D.; Hodgdon, M. L. 1985: On shear bands in ductile materials. Arch. Rat'l Mechs. Anal. 90: 219–247

Cosserat, E.; Cosserat, F. 1909: Théorie des Corps deformables. Hermann, Paris

de Borst, R.; Sluys, L. J. 1991: Localization in a Cosserat continuum under static and dynamic loading conditions. Comp. Meth. Appl. Mech. Eng. 90: 805–827

Dillon, Jr. O. D.; Kratochvil, J. 1970: A strain gradient theory of plasticity. Int. J. Solids and Structures 6: 1513–1533

Farren, W. S.; Taylor, G. I. 1925: The heat developed during plastic extrusion of metal. Proc. R. Soc. A107: 422

Green, A. E.; McInnis, B. C.; Naghdi, P. M. 1968: Elastic-plastic continua with simple force dipole. Int. J. Engng. Sci. 1: 373–394

Hinton, E.; Rock, T.; Zienkiewicz, O. C. 1976: A note on mass lumping and related processes in the finite element method. Earthquake Engng. and Structural Dynamics 4: 245–249

Hughes, T. J. R. 1987: The finite element method: linear static and dynamic finite element analysis. Prentice Hall, Englewood Cliffs, NJ

Massey, H. F. 1921: The flow of metal during forging. Proc. Manchester Assoc. Engrs., pp. 21–26

Mindlin, R. D. 1965: Second gradient of strain and surface tension in linear elasticity. Int. J. Solids and Structures. 1: 417–438

Seeger, A. 1957: In Dislocations and Mechanical Properties of Crystals, John Wiley

Sulijoadikusumo, A. U.; Dillon, Jr. O. W. 1979: Temperature distribution for steady axisymmetric extrusion with an application to Ti-6Al-4V. J. Thermal Stresses 2: 97

Toupin, R. A. 1962: Elastic materials with couple stresses. Arch. Rat'l Mechs. Anal. 11: 385–414

Tresca, H. 1978: On further application of the flow of solids. Proc. Inst. Mech. Engrs. 30: 301–345

Vardoulakis, I.; Aifantis, E. 1991: A gradient flow theory of plasticity for granular materials. Acta Mechanica 87: 197–217

Wright, T. W.; Batra, R. C. 1987: Adiabatic shear bands in simple and dipolar plastic materials. In: Kawata, K.; Shiori, J. (eds.) Macro- and Micro-Mechanics of high velocity deformation and fracture. IUTAM Symp. on MMMHVDF, Tokyo, Japan, Springer-Verlag, Berlin, Heidelberg, pp. 189–201

Zbib, H. M.; Aifantis, E. 1988: On the localization and postlocalization behavior of plastic deformation. I. On the initiation of shear bands. Res. Mechanica 23: 261–277

Zener, C.; Hollomon, J. H. 1944: Effect of strain rate upon plastic flow of steel. J. Appl. Phys. 15: 22–32